Ultrastable Low-Noise Current Amplifiers With Extended Range and Improved Accuracy

Dietmar Drung and Christian Krause

***Abstract*— The ultrastable low-noise current amplifier (ULCA) was developed as an advanced instrument for the improved measurement of currents generated by single-electron transport (SET) devices. It was optimized for direct currents in the picoampere range, and achieves an uncertainty of <0.1 μA/A for a current of 100 pA typically generated by SET pumps. This paper summarizes our efforts in extending the ULCA's current range and minimizing the measurement uncertainty over a wide range. Two ULCA variants with improved short-term uncertainty of about 0.02 μA/A or improved noise level of 1.4 fA/$\sqrt{\text{Hz}}$ are presented. Combining these devices allows the construction of a novel standard for direct currents below 50 μA, which has superior performance to previous methods for small-current generation or measurement. ULCAs involving thick-film resistors achieve noise levels down to 0.43 fA/$\sqrt{\text{Hz}}$. A low-bias variant features an effective input bias current within ±100 aA and a temperature coefficient within ±10 aA/K, which enables uncertainties below 10 aA in direct current measurements without reversing or switching ON/OFF the signal current.**

***Index Terms*— Calibration, current measurement, low-noise amplifiers, measurement standards, measurement uncertainty.**

I. Introduction

THERE is growing interest in the accurate measurement of small electric currents. In metrology, the development of single-electron transport (SET) devices requires current measurement with ultimate accuracy. Uncertainties of 0.1 ppm or better are desirable at direct currents of about 100 pA, typically generated by SET pumps [1]–[4]. For the calibration of picoamperemeters, e.g., in dosimetry or the semiconductor industry, there is need for accurate subnanoampere current generation. The traceable generation of small direct currents for calibration purposes is commonly performed at national metrology institutes with the capacitor charging method or with setups based on applying a voltage to a high-value resistor [5]–[10]. Uncertainties of about 10 ppm are achieved at best [10]; about 1 ppm is achievable with a 1-GΩ standard resistor calibrated with a cryogenic current comparator (CCC) [3].

The ultrastable low-noise current amplifier (ULCA) was recently introduced as an improved instrument for small direct currents [11]–[13]. Besides current measurement, it allows current generation as well as the calibration of high-value resistors with unmatched accuracy. It achieves uncertainties of about 0.1 μA/A at 100 pA and has a dynamic range of ±5 nA. At very small currents below about 1 pA, the total measurement uncertainty is typically dominated by the ULCA's input current noise of 2.4 fA/$\sqrt{\text{Hz}}$. This paper reports the current status of our work toward minimized uncertainty in an extended current range from ±50 μA down to the attoampere regime.

II. Effect of Resistor Nonlinearity

The ULCA involves two amplifier stages, the first (input stage) providing current amplification with gain $G_I = 1000$ and the second (output stage) performing a current-to-voltage conversion via a highly stable resistor $R_{IV} = 1$ MΩ. The resulting transresistance (output voltage versus input current) is $A_{\text{TR}} = G_I R_{IV} = 1$ GΩ. In the initial design, the 1000-fold current amplification is realized with a special network of about 3000 individual 2 MΩ chip resistors of size 0805 (2 mm × 1.25 mm), wired as a matched resistor pair of 3 GΩ and 3 MΩ [11]. As a result, this device (denoted in the following as "3 GΩ ULCA") features a noise level of 2.4 fA/$\sqrt{\text{Hz}}$ and a dynamic range of ±5 nA. A high-accuracy variant with 200 kΩ chip resistors was also realized [11]. It was supposed to lead to a corresponding improvement in the overall accuracy. However, the increased noise level of 7.5 fA/$\sqrt{\text{Hz}}$ (resulting from the tenfold reduction in total resistance to 300 MΩ) made this variant unattractive at the present phase, where noise typically limits the overall uncertainty in SET experiments.

A preliminary uncertainty budget for the 3 GΩ ULCA with conservative estimates of the uncertainty contributions was presented in [12]. According to the assumptions made, an uncertainty of about 0.06 μA/A is achievable if the ULCA is calibrated shortly before or after a measurement with PTB's 14-bit CCC (excluding the contribution of the voltmeter at the ULCA output) [14]. It turned out later that some of the quoted estimates were too conservative. For example, the CCC electronics is always operated with the battery chargers turned OFF when calibrating the ULCA. Therefore, the bounds for the error flux in the SQUID $\Delta\Phi$ can be reduced by a factor of 2 to $\pm 5 \times 10^{-7}\ \Phi_0$ (Φ_0 is the flux quantum). The settling after

Manuscript received July 7, 2016; revised September 2, 2016; accepted September 6, 2016. This work was supported in part by the Joint Research Project 15SIB08 e-SI-Amp. This project has received funding from the European Metrology Programme for Innovation and Research co-financed by the Participating States and from the European Union's Horizon 2020 research and innovation programme. The Associate Editor coordinating the review process was Dr. Francois Piquemal. *(Corresponding author: Dietmar Drung.)*

D. Drung is with the Physikalisch-Technische Bundesanstalt (PTB), 10587 Berlin, Germany (e-mail: dietmar.drung@ptb.de).

C. Krause is with the Physikalisch-Technische Bundesanstalt (PTB), 38116 Braunschweig, Germany (e-mail: christian.krause@ptb.de).

Color versions of one or more of the figures in this paper are available online at http://ieeexplore.ieee.org.

Digital Object Identifier 10.1109/TIM.2016.2611298

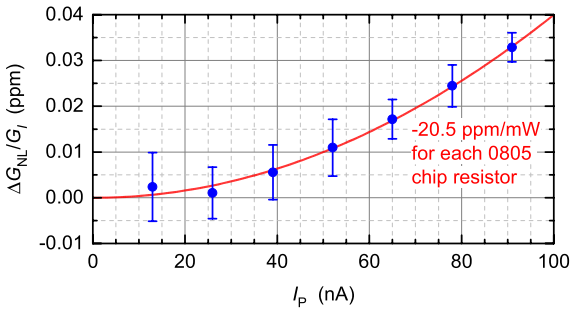

Fig. 1. Nonlinearity of a 300 MΩ network measured with the 14-bit CCC versus input current amplitude I_P. The current was reversed every 10 s, and the first 5 s after each reversal were disregarded. The data points represent the mean of 2–4 independent measurements taken with a sequence that reduces drift effects. At low currents, longer sampling times were chosen to lower the uncertainty, resulting in a total averaging time of nearly 9 h. Blue dots show measured data and the red solid line is a quadratic fit yielding a PCR of the individual size-0805 chip resistors of −20.5 ppm/mW. The chosen reference value for the gain nonlinearity ΔG_{NL} constrains the fit curve to pass through the origin. Error bars show type A standard uncertainties.

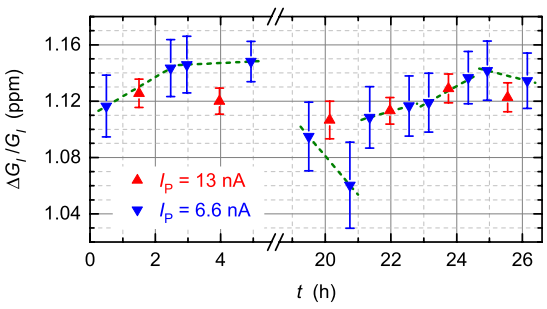

Fig. 2. Relative gain deviation $\Delta G_I/G_I$ of a 3 GΩ ULCA measured with the 14-bit CCC for two input current amplitudes $I_P = 6.6$ and 13 nA, respectively. The current was reversed every 10 s, and the first 5 s after each reversal were disregarded. A total of 18 measurements are plotted versus the mean time t of the measurement. The individual measurements took between 30 min and 1 h, resulting in a total sampling time of 10½ h. Dashed lines are linear fits through pairs of ±6.6 nA measurements placed time-symmetrically around the ±13 nA measurements. The nonlinearity is determined from the vertical offset between the dotted lines and the corresponding ±13 nA results. Error bars show type A standard uncertainties.

current reversal is also faster than previously assumed, allowing a reduction of the corresponding uncertainty component by a factor of 2 as well. However, these improvements do not noticeably reduce the overall uncertainty in the preliminary uncertainty budget, because it is dominated by the unknown nonlinearity effects in the ULCA's resistor network [12].

A discussion of resistor nonlinearity and first experimental results are presented in [15]. In the case of the 3 GΩ ULCA, the nonlinearity cannot be measured with sufficiently low random uncertainty, even if PTB's 14-bit CCC is used that exhibits a very low current noise level in the relevant frequency range. Therefore, the nonlinearity of a 300-MΩ network was investigated instead, taking advantage of the tenfold current range compared with the 3 GΩ variant. Fig. 1 shows the dependence of the relative nonlinearity error $\Delta G_{NL}/G_I$ on the peak input current I_P. The solid line is a quadratic fit from which a power coefficient of resistance (PCR) of −20.5 ppm/mW is deduced for the individual size-0805 chip resistors mounted on the network board. A mean temperature coefficient of resistance (TCR) of −9.5 ppm/K was determined by measuring the temperature dependence of the total resistance at the low-ohmic part of the network. This results in a thermal resistance of about 2.2 K/mW per chip resistor at the low-ohmic part (the power dissipation per resistor at the high-ohmic part is a factor of 1000 smaller and therefore neglected). In order to minimize the leakage currents, as much material as possible had been milled away from the printed circuit board carrying the resistors. This strongly reduces the cooling of the chip resistors and presumably causes the atypically high thermal resistance.

Applying the thermal model to the 3 GΩ network would reduce the contribution from resistor nonlinearity by a factor of 4.5 compared to our previous estimate, which relied on an assumed voltage coefficient within ±0.1 ppm/V. As a consequence, the total uncertainty of the 3 GΩ ULCA could be improved to about 0.04 μA/A. To check this prediction, the current gain of a 3 GΩ ULCA (channel A of the device reported in [13]) was calibrated with the 14-bit CCC alternately at ±6.6 and ±13 nA input current. Changing the current from ±6.6 to ±13 nA increases the power dissipation in each 2 MΩ resistor at the low-ohmic part of the network by 245 nW, leading to an expected temperature rise of 0.53 mK. Assuming a typical TCR of +10 ppm/K (estimated from measurements of resistor samples), this results in an expected gain change of −0.0053 ppm.

The measurement results are depicted in Fig. 2. Averaging the gain changes calculated from the six data triples taken over a period of two days with a total sampling time of 10½ h yields (−0.003 ± 0.008) ppm. This is consistent with the nonlinearity predicted from the thermal model, but is substantially smaller than the change of ±0.04 ppm expected for a voltage dependence of resistance of ±0.1 ppm/V (assumed as bounds in [12]). To prove the thermal model beyond doubt, the uncertainty has to be reduced by at least a factor of four, which would lead to very long sampling times of at least seven days even with the very good low-frequency noise performance of PTB's 14-bit CCC.

As a consequence of the findings, "high-current" ULCA variants (i.e., intended for currents above about 10 nA) should involve resistors with minimum TCR and should be designed with lower current gain to minimize nonlinearity from the temperature effects in the resistors. In fact, we started to develop ULCA variants with a 100-fold current gain for currents of up to ±1 μA with expected uncertainties approaching 0.01 μA/A. However, we stopped this development because in the nanoampere range, the highest accuracy can be achieved using the CCC directly for current measurement or generation. Furthermore, we found that the current range of the standard 3 GΩ ULCA can be increased to ±5 μA by a simple modification, which was first presented in [15] and will be described in detail in the following section.

III. ULCA Range Extension

For currents within the standard ±5 nA dynamic range, the 3 GΩ ULCA is operated conventionally with both the input and output stages [11]. To extend the dynamic range

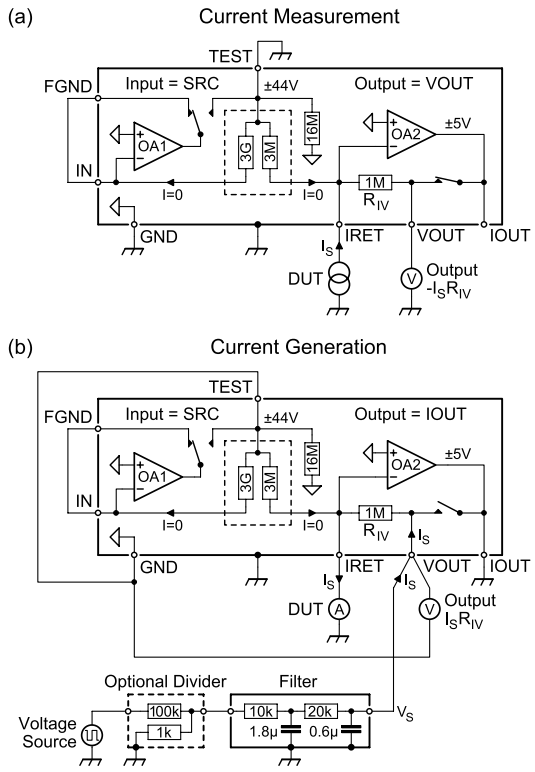

Fig. 3. Configurations for extending the current range of the 3 GΩ ULCA to ±5 μA. (a) Current measurement with a current source as DUT. (b) Current generation with an amperemeter as DUT. In (b) a star-shaped wiring for source voltage V_S and voltmeter is recommended to minimize the parasitic series resistance. A low-pass filter with a 3 dB cutoff frequency of 5.2 Hz and an optional voltage divider are used to suppress noise from the voltage source. The quoted voltage ranges of ±44 and ±5 V denote the nominal output ranges of the two ULCA stages.

from ±5 nA up to ±5 μA, the output stage can be applied without current amplification by the input stage, and the input stage is wired such that it does not affect the output signal. The corresponding configurations are depicted in Fig. 3. The current noise level is substantially increased to about 160 fA/$\sqrt{\text{Hz}}$ with a $1/f$ corner around 1 mHz. However, for high currents this is not an issue. At ±5 nA (the lowest current of the "extended mode"), the ULCA's contribution to the type A standard uncertainty is typically below 0.5 ppm for a measurement time of 1 h (not including the noise contribution of the voltmeter at the ULCA output).

In the case of current generation according to Fig. 3(b), the ULCA's 1 MΩ resistor is not connected to the output of amplifier OA2. The latter is grounded to form a servo loop that keeps the current output terminal IRET at internal ground potential (triangles in Fig. 3). This suppresses the burden voltage of the device under test (DUT) similar to the normal mode of operation involving both the ULCA stages [11].

Fig. 3 shows the configurations for current measurement and generation; however, resistance calibration can also be performed. For this, a calibrated voltage source in conjunction with the resistor to be calibrated is used to generate a current that is measured with the ULCA. Alternatively (preferably for lower resistances), the ULCA can be set into source mode and the generated current is passed through the resistor to be calibrated. The resulting voltage drop is measured with a calibrated voltmeter connected across the resistor.

The first measurements with the described range extension are presented in [16]. Throughout the investigated current range of 1 fA–1 μA, the uncertainties achieved with the 3 GΩ ULCA were below PTB's present calibration and measurement capabilities (CMCs). At small currents, the uncertainty was limited by the ULCA's noise and the relatively small transresistance of 1 GΩ. The latter can be increased to 100 GΩ using an external 100 MΩ resistor instead of the built-in 1 MΩ standard resistor [11]. We have implemented such a resistor by a series-connection of ten high-accuracy 10 MΩ chip resistors (±0.01% tolerance and ±5 ppm/K TCR). The device is housed in a small box with BNC connectors, and can be calibrated with the ULCA at the highest accuracy if necessary (see [13, Fig. 1]).

IV. Second ULCA Generation

Based on the results presented above and on two years of experience with the standard 3 GΩ ULCA, a second generation with four main variants was developed (see Table I). For the input stage networks, the resistor size was increased from 0805 to 1206 (3.2 mm × 1.6 mm). The network boards were designed such that a damaged resistor can be localized by ohmmeter measurements without unsoldering components. In contrast to that, for the first-generation network, resistor problems at the low-ohmic part can only be narrowed down to groups of 32 parallel-connected resistors, so that up to 32 resistors have to be unsoldered to repair a faulty board.

Two network types with different resistor configurations and current gains G_I = 1000 or 100 000 were developed. The 1000-fold gain is realized by a 1000s/30s30p configuration, i.e., the high-ohmic part consists of 1000 resistors connected in series, while the low-ohmic part is implemented by a series/parallel connection of 30 × 30 = 900 resistors. The individual chip resistors have 1, 10, or 100 MΩ which yields total resistances of 1, 10, or 100 GΩ at the high-ohmic part, respectively. For comparison, the standard 3 GΩ ULCA involves 2 MΩ resistors in a 1500s/48s32p configuration. The resistor network with a 100 000-fold gain was developed to achieve the lowest possible input bias current at the expense of degraded accuracy.

The short-term uncertainties in Table I indicate the standard uncertainties achievable within one day after calibration. They are estimates of the expected performance and include the effects of short-term fluctuations and nonlinearity in the ULCA's transresistance. For longer periods between calibration and measurement, the long-term drift component has to be included. For the 3 GΩ ULCA with size-0805 resistors, an initial drift of typically 5 ppm/year was observed [11]. The drift was found to decrease with time. One or two years after assembling, it dropped to about 2 or 1 ppm/year, respectively.

The high-accuracy and low-noise variants involve thin-film resistors (NiCr or CrSi). The resistor networks are tailored for the highest accuracy or the lowest noise, respectively. The low-noise ULCA is intended as an improved replacement of the 3 GΩ ULCA for the characterization of SET devices.

TABLE I
SECOND-GENERATION ULCA VARIANTS IN COMPARISON WITH THE STANDARD 3 GΩ ULCA

ULCA variant	3 GΩ standard	1 GΩ high-accuracy	10 GΩ low-noise	100 GΩ low-current	175 GΩ low-bias
Chip resistors					
Configuration	1500s/48s32p	1000s/30s30p	1000s/30s30p	1000s/30s30p	175s/2s1143p
Chip size	0805	1206	1206	1206	1206
Technology	NiCr	NiCr	NiCr or CrSi	Thick-film	Thick-film
Value (MΩ)	2	1	10	100	1000
Tolerance (%)	±0.1	±0.01	±0.1	±1	±1
TCR (ppm/K)	±25	±5	±50	±100	±100
Nominal input gain G_I	1000	1000	1000	1000	100 000
Output R_{IV} (MΩ)	1	0.1	1	10	10
Total A_{TR} (GΩ)	1	0.1	1	10	1000
Input resistance R_{TEST} (MΩ)	2.524	0.8268	3.24	4.58	1.6
Noise @ 0.1 Hz (fA/√Hz)	2.4	4.1	1.4	0.6	0.43
1/f corner (μHz)	400	1500	600	150	50
Current range (nA)	±5	±44	±4.4	±0.44	±0.005
Eff. input bias $I_{\mathrm{B,eff}}$ (fA)	±30	±100	±3	±2	±0.1
Temp. coeff. of $I_{\mathrm{B,eff}}$ (fA/K)	±1	±3	±0.2	±0.2	±0.01
Expected short-term standard uncertainty (μA/A)	0.04	0.02	0.1	1	10

With improved cryogenic wiring [17], the reduced ULCA noise level of 1.4 fA/$\sqrt{\mathrm{Hz}}$ allows a substantial reduction in measurement time while still achieving about 0.1 μA/A overall standard uncertainty.

The improved ULCA networks rely on high-value thin-film resistors that are at the limit of the manufacturers' fabrication capabilities. For the development, in order to check the resistor suitability, we typically start with test networks involving only a small number of resistors from different manufacturers. For example, the network of the low-noise ULCA was originally intended to be made from 20 MΩ CrSi resistors in a 600s/24s40p configuration, yielding a total resistance of 600×20 MΩ $= 12$ GΩ. Because these parts were not available from stock, we first investigated a test network with 10 MΩ resistors from the same series (P-Series from Vishay Sfernice), which showed excellent noise and stability. However, it turned out that the 20 MΩ resistors exhibit much higher resistance fluctuations than the 10 MΩ parts, which would limit the short-term uncertainty of the low-noise ULCA to about 0.4 μA/A. The difference in quality could result from different fabrication technologies: since the manufacturer specification "NiCr or CrSi" is rather undefined, it is possible that the 10 MΩ resistors are fabricated in NiCr technology, being superior to the 20 MΩ made from CrSi. Therefore, we finally decided to use the 10 MΩ resistors and changed the network configuration to 1000s/30s30p, which yields 1000×10 MΩ $= 10$ GΩ for the low-noise ULCA.

For the highest demands, e.g., for high-accuracy measurements of currents generated by SET pumps [4] or for the quantum metrology triangle experiment [18], the short-term uncertainty of the low-noise ULCA can be further improved by calibrating its input gain with a high-accuracy ULCA instead of the CCC directly. The corresponding setup is shown in Fig. 4. It is similar to the self-test configuration in [11, Fig. 4]. The voltage output $I_{\mathrm{S}} \Delta G_I R_{IV}$ is measured with a voltmeter, where I_{S} is the calibration current, ΔG_I is the difference between the current gains of the two ULCA input stages, and $R_{IV} = 1$ MΩ is the output transresistance of the low-noise ULCA calibrated separately with the CCC. The demands on the voltmeter accuracy are quite modest because the relative current gain difference $\Delta G_I / G_I$ is small, typically below 100 ppm.

Using the high-accuracy ULCA for calibration instead of the CCC reduces the effective uncertainty contribution from SQUID nonlinearity in the calibration chain [12]. This results from the fact that the high-accuracy ULCA is calibrated with the CCC at a high current of ±31 nA that substantially exceeds the ±4.4 nA dynamic range of the low-noise ULCA. The resulting SQUID nonlinearity contribution is correspondingly reduced. In spite of the high current range of the high-accuracy ULCA, the uncertainty contribution from resistor nonlinearity according to the thermal model presented in Section II is sufficiently low (0.0034 ppm calculated for a thermal resistance of 1.1 K/mW estimated for the size-1206 chip resistors). Furthermore, the noise level of the high-accuracy ULCA is lower than that of the 14-bit CCC at frequencies below about 0.1 Hz [12].

In Fig. 4, the source voltage is applied to the TEST connector via a filter. The resistance against ground R_{TEST} loads the filter and reduces the effective source voltage V_{S} correspondingly. However, this does not affect the calibration accuracy because the actual current I_{S} can be measured separately with the high-accuracy ULCA by removing the cable between the two IRET connectors and setting the output amplifier OA2 from OFF to V_{OUT} mode. Using the known transresistance A_{TR} of the high-accuracy ULCA, the calibration current can

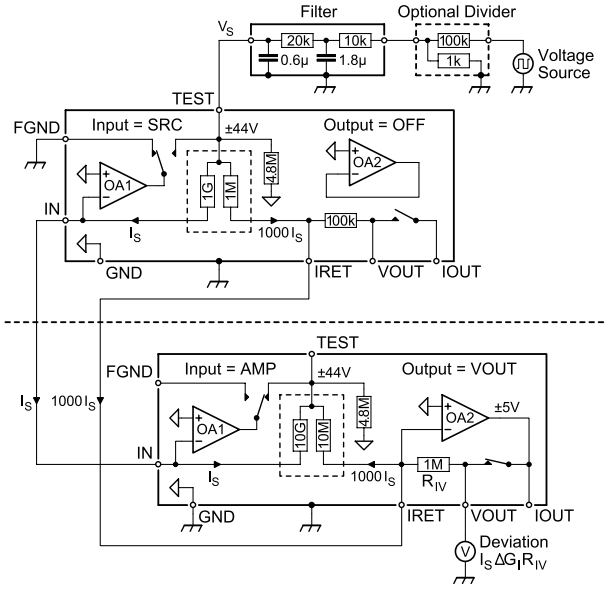

Fig. 4. Improved calibration of the input current gain G_I of the low-noise ULCA. A calibrated high-accuracy ULCA (drawn above the dashed line) is used to generate the signals driving the ULCA to be calibrated (drawn below the dashed line). A low-pass filter with a 3-dB cutoff frequency of 5.2 Hz and an optional voltage divider are used to suppress noise from the voltage source. The voltage V_S is selected to obtain the desired calibration current I_S. The output signal $I_S \Delta G_I R_{IV}$ is measured with a voltmeter. The electrical connections between the housings via the cable shields are omitted for clarity.

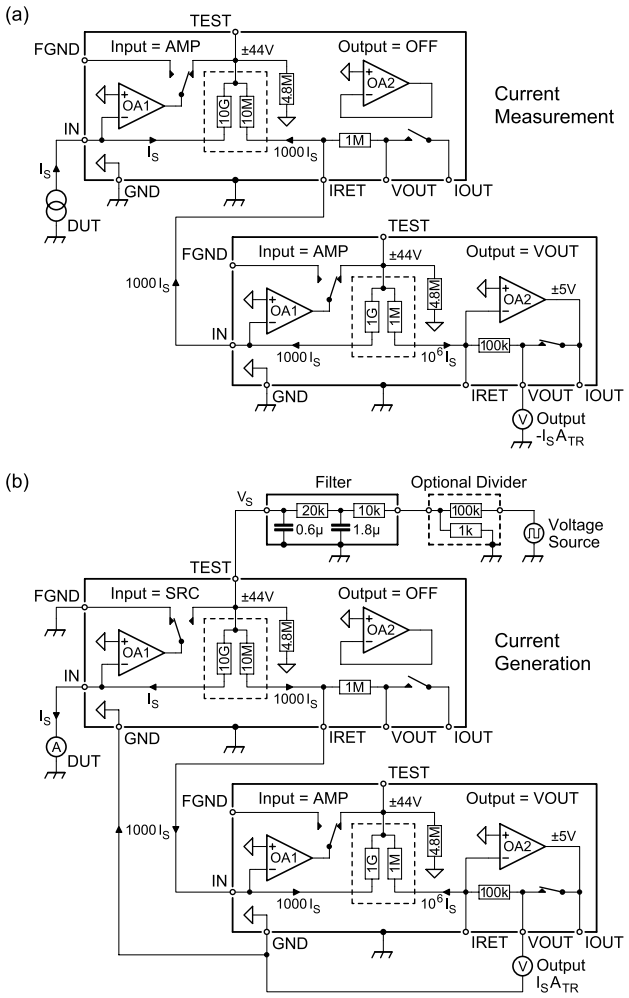

Fig. 5. ULCA cascade for (a) current measurement and (b) current generation. The DUT is indicated by a current source or an amperemeter, respectively. In the case of current generation, a low-pass filter with a 3 dB cutoff frequency of 5.2 Hz and an optional voltage divider are used to suppress noise from the voltage source. The electrical connections between the housings via the cable shields are omitted for clarity.

be determined from the measured output voltage as $I_S = V_{OUT}/A_{TR}$.

The input resistances R_{TEST} are listed in Table I for the various ULCA variants. They include the contributions of the corresponding guard circuits, which is considered in the circuit diagrams by an extra resistor between TEST and internal ground (16 MΩ for the 3 GΩ standard ULCA and 4.8 or 18 MΩ for the new boards with $G_I = 1000$ or 100 000, respectively).

At currents below 44 pA, the low-noise and high-accuracy ULCAs can be cascaded to increase the overall transresistance. As shown in Fig. 5, cascading is possible for current measurement as well as for current generation. The low-noise ULCA serves as a current preamplifier. Its output stage is deactivated, and the amplified current is passed through the IRET connector into the input of the high-accuracy ULCA. The high total transresistance $A_{TR} = 1000 \times 100$ MΩ $= 100$ GΩ and the resulting high output voltage $\pm I_S A_{TR}$ simplifies the metering of the ULCA's output signal. In the case of current generation, a servo loop involving amplifier OA1 of the low-noise ULCA is used to suppress the burden voltage of the DUT [11].

The amplifiers OA1 and OA2 have extremely high open-loop gains well above 10^9 [13]. The devices used in the ULCA are complex circuits involving several monolithic operational amplifiers and a high-voltage output stage with discrete components (for a more detailed schematic see [11, Fig. 5]). The front-end amplifier in the input stage determines the overall current noise and input bias current. For the standard 3 GΩ ULCA, the LTC6240 from Linear Technology was chosen. Recently, the ADA4530-1 from Analog Devices became available which has a subfemtoampere input bias current thanks to an improved amplifier design. For high resistance values, this device is superior to the LTC6240. Therefore, it is used for all second-generation ULCAs except the high-accuracy variant.

An important ULCA application is the calibration of amperemeters and current sources. Using the low-noise and high-accuracy ULCAs individually or as a cascade, a highly accurate current standard for both current sourcing and metering can be realized for a very wide current range of up to ±50 μA. The expected uncertainties of this novel instrument between 1 fA and 10 μA are summarized in Table II. Above 44 pA the best-suited ULCA is selected, whereas below 44 pA both the ULCAs are cascaded. As described above, in the ULCA cascade the low-noise ULCA (called G_I device in Table II) is applied as preamplifier for the high-accuracy ULCA (the I/V device) performing the current-to-voltage conversion. For all currents in Table II and Fig. 6, the predicted uncertainties are lower than with the calibration setups currently used at PTB (see CMC entries in the right column of Table II). Furthermore, the uncertainties and/or measurement

TABLE II

PREDICTED UNCERTAINTY OF A DIRECT CURRENT STANDARD BASED ON TWO SECOND-GENERATION ULCAS

Current (A)	G_I device (Ω)	I/V device (Ω)	Total A_{TR} (Ω)	Time τ (h)	Uncertainty (ppm)	CMC (ppm)
±1 f	10 G	1 G	100 G	7	20000	60000
±10 f	10 G	1 G	100 G	7	2000	6000
±100 f	10 G	1 G	100 G	7	200	360
±1 p	10 G	1 G	100 G	7	20	85
±10 p	10 G	1 G	100 G	7	2 (3)	75
±100 p	—	10 G	1 G	7	0.5 (2)	20
±1 n	—	10 G	1 G	1	0.4 (2)	60
±10 n	—	1 G	100 M	<1	0.4 (2)	60
±100 n	—	10 G	1 M	<1	0.4 (2)	60
±1 µ	—	10 G	1 M	<1	0.4 (2)	20
±10 µ	—	1 G	100 k	<1	0.4 (2)	3

Combined expanded uncertainties ($k = 2$) are quoted that include type B effects from calibration of the equipment shortly before and/or after a measurement. Uncertainties for quarterly calibration are given in parentheses if they are noticeably higher. For the instrument to be calibrated an ULCA is assumed; its uncertainty contribution is also included. For the voltmeters, a short-term uncertainty of 0.2 ppm ($k = 2$) and a drift within ±4 ppm/yr were assumed. For currents below 44 pA, a cascade of two ULCAs is used to increase the total transresistance to 100 GΩ. Above 44 nA, the extended mode is applied. For comparison, PTB's present CMCs are also shown [19].

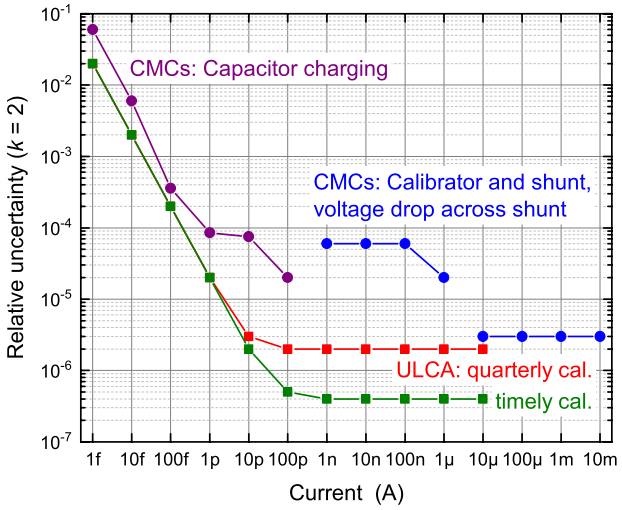

Fig. 6. Graphical illustration of the data in Table II.

times are reduced compared with the initial approach of using the standard 3 GΩ ULCA only [16].

Two ULCAs involving thick-film resistors (classified in Table I as 100 GΩ low-current and 175 GΩ low-bias variants) were also realized to obtain the highest possible resistances. The resulting low input bias currents and $1/f$ corner frequencies make these variants well suited for direct current measurements in the femtoampere range. Thick-film resistors from different manufacturers (having different tolerances and TCRs) were investigated. In contrast to thin-film elements, thick-film resistors show relatively high levels of $1/f$ resistance fluctuations (commonly called "resistor noise" or "current noise"). This leads to degraded short-term stability

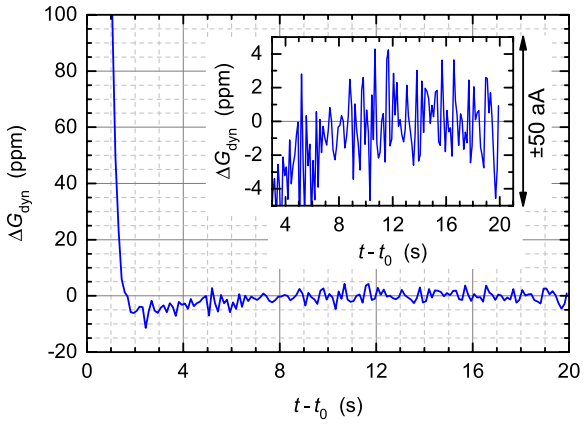

Fig. 7. Settling behavior of the current gain G_I of a low-bias ULCA. ΔG_{dyn} is the relative deviation of G_I from its final value after decaying of transients, and t–t_0 is the time after current reversal. A trapezoidal test current of ±5 pA with a ramp time of 0.1 s was applied to the ULCA input via a 10 GΩ resistor. The ULCA output was digitized with 256 samples per second (i.e., well above its 3 dB bandwidth of about 23 Hz), and the noise was reduced using the mean values of 32 samples for further processing. 16 640 individual step responses were averaged. The responses to the positive current steps were directly used for averaging, whereas those for the negative steps were inverted before taking them into account. The inset shows a magnification of the final settling with relative and absolute ranges of ±5 ppm and ±50 aA, respectively.

and correspondingly increased short-term uncertainties [13]. Furthermore, thick-film resistors exhibit a relatively strong voltage coefficient of resistance (VCR) which substantially exceeds the nonlinearity from thermal effects found dominant in the ULCA's thin-film resistors (see Section II). The short-term uncertainties of the low-current and low-bias variants are markedly affected by the VCR of the resistive elements, which was estimated from measurements of small test networks. A detailed study of the nonlinearity of ULCAs with complete thick-film resistor boards is planned for the near future to determine the short-term uncertainties typically achievable in practice.

For noise and linearity reasons, the input stage of the 100 GΩ ULCA is calibrated with the 10 GΩ variant equivalently to the circuit depicted in Fig. 4. Due to the very high current gain of the low-bias ULCA exceeding the number of turns in our CCC, a direct calibration with CCC is not possible. The total transresistance A_{TR} of this device is therefore calibrated using the ULCA cascade described above (see Table II).

For the high-ohmic ULCA variants, the settling after current reversal turned out to be crucial. The new resistor boards were carefully optimized with respect to fast settling. Fig. 7 shows as example the settling behavior of the input stage of a low-bias ULCA. In spite of the high network resistance of nominally 175 GΩ, the device settles to within ±5 ppm after about 4 s. Note that the noise in Fig. 7 is dominated by thermal noise in the 10 GΩ resistor used to generate the ±5 pA test current.

The low-bias ULCA is tailored for extremely small direct currents without the need for reversing or switching ON/off the current to suppress drift effects. It features an exceptionally low effective input bias current $I_{B,eff}$ of typically within ±100 aA, which has a temperature coefficient within ±10 aA/K. Note that $I_{B,eff}$ results from the superposition of

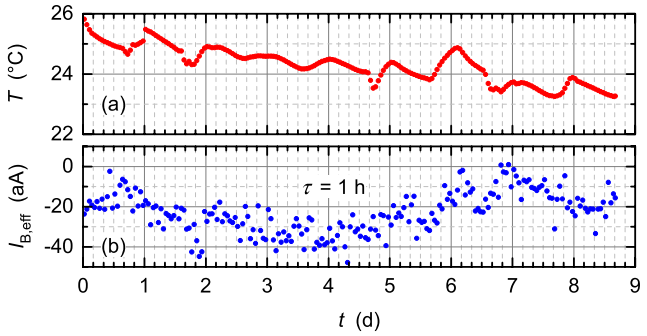

Fig. 8. (a) Temperature T and (b) effective input bias current $I_{B,eff}$ of a low-bias ULCA measured over a period of nearly nine days. Each data point shows the mean value over a sampling time $\tau = 1$ h.

four effects, caused by the bias current and the offset voltage of input stage amplifier OA1 and of output stage amplifier OA2, respectively [17]. Thanks to the high current gain of 100 000, the effect of the bias current of OA2 is strongly suppressed. The contributions of the offset voltages of OA1 and OA2 decrease with increasing resistance of the resistor network. For 175 GΩ, the offset voltage of OA1 typically causes the largest contribution. Therefore, we plan to test the low-bias ULCA with a higher resistance of 350 GΩ, realized by 2 GΩ chip resistors with ±2% tolerance and ±300 ppm/K TCR. Measurements with resistances above 175 GΩ have not yet been performed because of the long lead times of the chosen 2 GΩ chip resistors.

Fig. 8 shows the measured input bias current of a low-bias ULCA. It was determined from the output voltage measured with open amplifier input: $I_{B,eff} = V_{OUT}/A_{TR}$. To eliminate the effect of external interference, the input connector was covered by a cap. The input bias current fluctuated around −20 aA with no clear drift over the measurement interval of nearly nine days. The temperature was also monitored using the ULCA's internal temperature sensor [11]. There is no noticeable correlation between the temperature and bias current fluctuations, i.e., temperature effects are negligible at a level of ±10 aA even in an environment with temperature fluctuations of a few degrees centigrade.

V. Conclusion

The ULCA is a user-friendly and superior alternative to existing meter and source instruments for small direct currents. It outperforms commercial devices and calibration setups used in metrology institutes by up to two orders of magnitude in accuracy. The standard 3 GΩ ULCA was originally optimized for dc currents in the picoampere range, but has proven to be well suited in a much wider range between about 1 fA and 5 μA. A second ULCA generation with four variants was developed to further extend the current range and to improve the accuracy. Uncertainties down to 0.02 ppm are expected for the high-accuracy variant in the nanoampere range. At smaller currents, the improved noise levels of the low-noise and low-current variants enable reduced measurement uncertainties. The low-bias ULCA combines the best noise level of about 0.43 fA/$\sqrt{\text{Hz}}$ with a very low $1/f$ corner frequency of about 50 μHz. Thanks to its small and stable input bias current, it allows uncertainties below 10 aA without reversing or switching ON/OFF the signal current. The presented developments are expected to set new accuracy benchmarks in the small-current regime.

Acknowledgment

The authors would like to thank M. Piepenhagen and M. Luther for fabrication and assembling of printed circuit boards, M. Götz, E. Pesel, and U. Becker for CCC calibrations, and H. Scherer for stimulating discussions.

References

[1] J. P. Pekola *et al.*, "Single-electron current sources: Toward a refined definition of the ampere," *Rev. Mod. Phys.*, vol. 85, no. 4, pp. 1421–1472, Oct. 2013.

[2] B. Kaestner and V. Kashcheyevs, "Non-adiabatic quantized charge pumping with tunable-barrier quantum dots: A review of current progress," *Rep. Prog. Phys.*, vol. 78, no. 10, p. 103901, Sep. 2015.

[3] S. P. Giblin *et al.*, "Towards a quantum representation of the ampere using single electron pumps," *Nature Commun.*, vol. 3, Jul. 2012, Art. no. 930.

[4] F. Stein *et al.*, "Validation of a quantized-current source with 0.2 ppm uncertainty," *Appl. Phys. Lett.*, vol. 107, no. 10, p. 103501, Sep. 2015.

[5] G.-D. Willenberg, H. N. Tauscher, and P. Warnecke, "A traceable precision current source for currents between 100 aA and 10 pA," *IEEE Trans. Instrum. Meas.*, vol. 52, no. 2, pp. 436–439, Apr. 2003.

[6] H. E. van den Brom, P. de la Court, and G. Rietveld, "Accurate subpicoampere current source based on a differentiating capacitor with software-controlled nonlinearity compensation," *IEEE Trans. Instrum. Meas.*, vol. 54, no. 2, pp. 554–558, Apr. 2005.

[7] L. Callegaro, V. D'Elia, P. P. Capra, and A. Sosso, "Techniques for traceable measurements of small currents," *IEEE Trans. Instrum. Meas.*, vol. 56, no. 2, pp. 295–299, Apr. 2007.

[8] N. E. Fletcher, S. P. Giblin, J. M. Williams, and K. J. Lines, "New capability for generating and measuring small DC currents at NPL," *IEEE Trans. Instrum. Meas.*, vol. 56, no. 2, pp. 326–330, Apr. 2007.

[9] T. Bergsten, K.-E. Rydler, O. Gunnarsson, G. Eklund, and V. Tarasso, "A precision current source using $\Delta-\Sigma$ Modulation," *IEEE Trans. Instrum. Meas.*, vol. 60, no. 7, pp. 2341–2346, Jul. 2011.

[10] G.-D. Willenberg, "EUROMET.EM-S24: Supplementary comparison of small current sources," *Metrologia*, vol. 50, no. 1A, p. 01002, 2013.

[11] D. Drung, C. Krause, U. Becker, H. Scherer, and F. J. Ahlers, "Ultra-stable low-noise current amplifier: A novel device for measuring small electric currents with high accuracy," *Rev. Sci. Instrum.*, vol. 86, no. 2, p. 024703, Feb. 2015.

[12] D. Drung, M. Götz, E. Pesel, and H. Scherer, "Improving the traceable measurement and generation of small direct currents," *IEEE Trans. Instrum. Meas.*, vol. 64, no. 11, pp. 3021–3030, Nov. 2015.

[13] D. Drung *et al.*, "Validation of the ultrastable low-noise current amplifier as travelling standard for small direct currents," *Metrologia*, vol. 52, no. 6, pp. 756–763, Oct. 2015.

[14] M. Götz, E. Pesel, and D. Drung, "A compact 14-bit cryogenic current comparator," in *29th Conf. Precis. Electromagn. Meas. Dig.*, Rio de Janeiro, Brazil, Aug. 2014, pp. 684–685.

[15] D. Drung and C. Krause, "Ultrastable low-noise current amplifiers with extended range and improved accuracy," in *30th Conf. Precis. Electromagn. Meas. Dig.*, Ottawa, ON, Canada, Jul. 2016, pp. 1–2.

[16] H. Scherer, D. Drung, and C. Krause, "Improved calibration of instruments for small direct currents," in *30th Conf. Precis. Electromagn. Meas. Dig.*, Ottawa, ON, Canada, Jul. 2016, pp. 1–2.

[17] C. Krause and D. Drung, "Measurement of sub-picoampere direct currents with uncertainties below ten attoamperes," *Rev. Sci. Instrum*, to be published.

[18] H. Scherer and B. Camarota, "Quantum metrology triangle experiments: A status review," *Meas. Sci. Technol.*, vol. 23, no. 12, p. 124010, Dec. 2012.

[19] Bureau International des Poids et Mesures (BIPM). (Aug. 2013). *Calibration and Measurement Capabilities Electricity and Magnetism*. [Online]. Available: http://kcdb.bipm.org/AppendixC/country_list_search.asp?CountSelected=DE&sservice=EM/DC.3.2

Dietmar Drung was born in Mühlacker, Germany, in 1958. He received the Dipl.-Ing. and Dr.-Ing. degrees in electrical engineering from the University of Karlsruhe, Karlsruhe, Germany, in 1982 and 1988, respectively.

He was a Researcher with the University of Karlsruhe from 1983 to 1988. In 1988, he joined Physikalisch-Technische Bundesanstalt, Berlin, Germany, where he was involved in superconducting quantum interference devices (SQUIDs) and SQUID readout electronics. In 2009, he was appointed as the Senior Scientist in Superconducting Sensors. His current research interests include the development of low-noise amplifiers and measurement systems for magnetic sensing and electrical metrology.

Christian Krause was born in Bad Salzungen, Germany, in 1985. He received the Dipl.-Ing. (Fachhochschule) degree in technical physics from the Brandenburg University of Applied Science, Brandenburg, Germany, in 2010, and the M.Sc. degree from the University of Cottbus, Cottbus, Germany, in 2013. He is currently pursuing the Ph.D. degree with the Technical University of Braunschweig, Braunschweig, Germany.

He was with Innovations for High Performance Microelectronics, Frankfurt, Germany, from 2010 to 2013, where he was involved in the reliability of microelectromechanical systems. In 2013, he joined Physikalisch-Technische Bundesanstalt, Berlin, Germany, where he is involved in the development of high precision amplifiers.